Jesse M. Teo, Campbell J. Coghlan, Jack D. Evans, Ehud Tsivion, Martin Head-Gordon, Christopher J. Sumby, and Christian J. Doonan
Hetero-bimetallic metal-organic polyhedra
Chemical Communications, 2016; 52(2):276-279

Published at: http://dx.doi.org/10.1039/c5cc08336b

ChemComm

COMMUNICATION

Hetero-bimetallic Metal-organic Polyhedra

Jesse. M. Teo,[a] Campbell J. Coghlan,[a] Jack D. Evans,[a] Ehud Tsivion,[b] Martin Head-Gordon,[b] Christopher J. Sumby*[a] and Christian J. Doonan*[a]

Received 00th January 20xx,
Accepted 00th January 20xx

DOI: 10.1039/x0xx00000x

www.rsc.org/

Porous metal-organic polyhedra (MOPs), constructed from heterometallic Pd^{II}-M^{II} (M = Cu, Ni, Zn) paddlewheel nodes and 5-*tert*-butyl-1,3-benzenedicarboxylate organic links, were prepared in which the Pd^{II} ions preferentially line the inner surface of the cage molecules. Careful activation produces co-ordinatively unsaturated 3d transition metal sites on the external MOP surfaces giving rise to H_2 binding energies in excess of 12 kJ/mol.

Porous materials, such as metal-organic frameworks (MOFs) and their discrete counterparts metal-organic polyhedra (MOPs), that are constructed from co-ordinatively unsaturated inorganic nodes show great potential for application to gas adsorption/separation processes, catalysis, and emerging opportunities in electronics, optics, sensing and biotechnology.[1] A salient example is the M_2(dobdc) (dobdc^{4-} = 2,5-dioxido-1,4-benzenedicarboxylate family of MOFs that possess 1D pore channels lined with a high density of open metal sites including Mg, Mn, Fe, Co, Ni, Zn.[2] Detailed theoretical and structural studies confirm that the exceptionally high affinities these materials exhibit towards gas molecules, such as H_2 and CO_2, originate from orbital and coulombic interactions between the adsorbate and the vacant coordination site of the metal oxide node.[3] In addition the dicopper paddlewheel node of HKUST-1 represents how accessible open metal sites can be exploited as Lewis acid catalysts.[4, 5]

Although structurally well-defined, co-ordinatively unsaturated metal sites in molecular complexes are a rich source of fundamental research, they are relatively uncommon in porous framework materials.[6, 7] Accordingly, novel porous solids comprised of such moieties are of significant interest to chemists. The metal paddlewheel unit is a common structural building block in porous framework materials due to its facile synthesis and topologically versatile square planar geometry.[8] Furthermore, the intrinsic vacant coordination sites have been used as a structural connection,[9] explored for their potential to enhance gas adsorption,[10] and heterogeneous catalysis.[11, 12] The most prevalent paddlewheel building unit for the synthesis of frameworks is based on Cu^{II}, however, Ni, Mo, Zn, Ru and Rh paddlewheel nodes have also been reported.[13-17] In an effort to expand the functional diversity of this common building block researchers have used a cation exchange approach to introduce extraneous metals into the paddlewheels of copper based MOFs.[18] Though this post-synthetic strategy was proven to be successful, if it can be achieved, the direct synthesis of materials offers more control over their composition and eliminates the need for additional synthetic steps that can result in degradation of the material.[19]

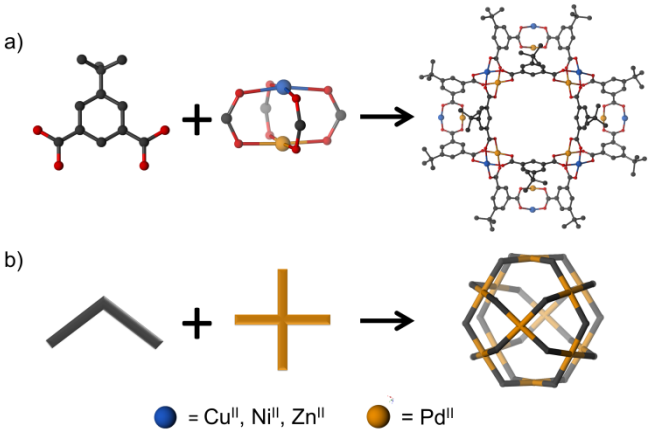

Figure 1. a) Structural and b) schematic representations of the synthesis of the cuboctahedral bimetallic MOPs, which contain 12 heteronuclear paddlewheel nodes, from Pd(μ-OAc)$_4$M(OH$_2$) and 5-*tert*-butyl-1,3-benzenedicarboxylic acid (H_2L). In the resulting MOP, the Pd^{II} sites are preferentially positioned within the void cavity, while the divalent first row transition metal occupies the external sites.

Here we describe the synthesis and characterisation of a series of porous metal-organic polyhedra constructed from bimetallic paddlewheels that are, hitherto, unprecedented building blocks for framework materials. The bimetallic metal units are based on a Pd^{II}–M^{II} (M = Ni, Cu or Zn) motif (Figure 1), where the Pd^{II} ions predominantly reside on the interior of the

[a] Centre for Advanced Nanomaterials, School of Physical Sciences, University of Adelaide, Adelaide, SA 5005, Australia.
[b] Department of Chemistry, University of California Berkeley, Berkeley, California 94720, United States.

Electronic Supplementary Information (ESI) available: synthetic procedures, single crystal and powder X-ray diffraction data, gas adsorption data and computational data. See DOI: 10.1039/x0xx00000x

cuboctahedral cages. As a consequence, the surface of the MOP can be selectively decorated with a series of first row transition metals that can be reacted to provide open coordination sites. We exploit this feature and determine the gas adsorption properties of these unique materials experimentally, using a theoretical analysis to further explain the adsorption. Notably, they show exceptionally high uptake of hydrogen for discrete porous molecules.

The bimetallic MOPs were synthesized by mixing 5-*tert*-butyl-1,3-benzenedicarboxylic acid (H_2L) and a precursor hetero-bimetallic paddlewheel acetate Pd^{II}–M^{II} (M = Ni, Cu or Zn)[20] in *N,N*-dimethylacetamide (DMA) at ambient temperature for 48 hrs under dry, anaerobic, conditions (20 days for M=Ni). This procedure afforded single crystals of the three Pd-M(L) MOPs that were suitable for X-ray diffraction studies. These new mixed-metal MOPs are isostructural with a number of known $Cu_2(L')$ analogues (L' = 5-hydroxy-1,3-benzenedicarboxylate and 5-*tert*-butyl-1,3-benzenedicarboxylate) and crystallise in the tetragonal space *I*4/*m* with two complete cage moieties in the unit cell.

Close analysis of the crystal structures obtained indicate that each MOP is best described by a cuboctahedral geometry with bimetallic paddlewheel units at 12 of the faces. The Pd^{II} and M^{II} ions, predominantly, adopt the endo- and exo-hedral positions of the 12 faces, respectively. The observed, systematic, distribution of metals can be explained by (i) a stepwise ligand exchange process that incorporates preformed bimetallic paddlewheel acetate into the MOP and (ii) the strong preference of d^8 Pd complexes towards square planar geometry; which can be accommodated at the endohedral sites of the MOP with least strain.[21] Ni, Cu and Zn are more co-ordinatively flexible, adopting 5-coordinate geometries in the presence of co-ordinating solvents, and thus favour the exohedral positions.[22, 23] Indeed, the first row transition metals manifest significant distortions from square planar geometry that are most apparent in the Pd^{II}–Zn^{II} MOP which exhibits a O–Zn–O bond angle of 165.6° and least pronounced in the Pd^{II}–Ni^{II} structure which has a O–Ni–O bond angle of 171.2° (SI Table 2). The distortions of the peripheral 3d metal sites in these materials compare favourably with the O–Cu–O angles for the $Cu_2(L)$ MOP, which are the range 168.1–168.6°, and further explains why the Pd^{II}–M^{II} MOP structure is identical to previously reported $Cu_2(L')$ MOPs. Notably, the Pd centres can be accommodated on the endohedral surface without significant changes in the overall MOP structure.

Each bimetallic paddlewheel presents short intermetallic distances in the range of 2.46–2.56 Å (SI Table 3). As expected, density functional theory (DFT) calculations of the paddlewheel cluster suggest the short metal-metal distances are due to geometric constraints imposed by the bridging carboxylate groups rather than a result of metal-metal bonding.[24] To satisfy the crystallographically assigned distribution of metals in the paddlewheel moieties a 1:1 Pd:M ratio is required. Energy-dispersive X-ray spectroscopy (EDX) was used to assess the metal composition for each MOP (SI Table 1). For the PdZn(L) and PdNi(L) MOPs the anticipated Pd:M ratio of 1:1 was confirmed, however, for the CuPd(L)

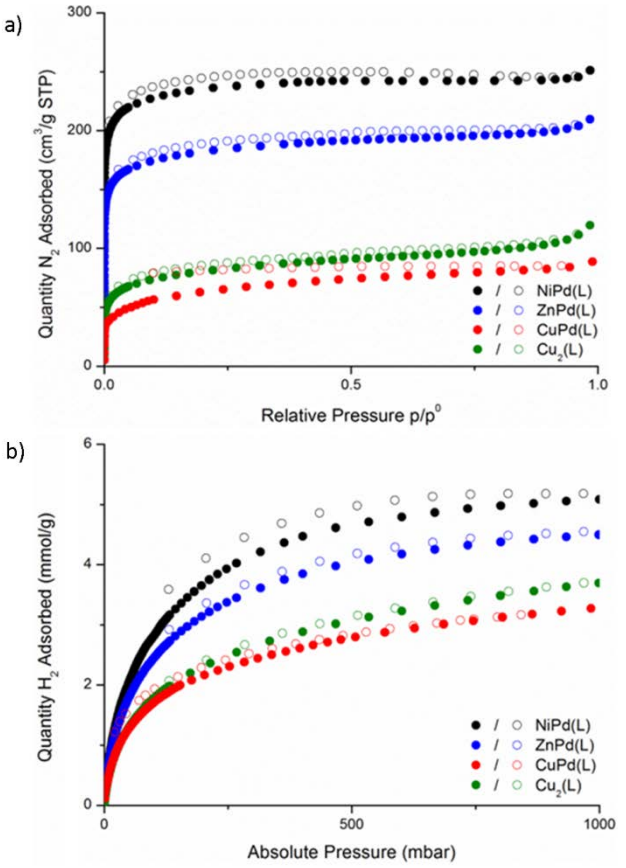

Figure 2. a) 77 K N_2 and b) H_2 adsorption isotherms for the hetero-bimetallic MPd(L) and Cu_2(L) MOPs following activation. Closed and open symbols represent adsorption and desorption data, respectively.

analogue the metal ratio heavily skewed towards Cu (62:38). This disparity in metal composition may be explained by the chemistry of the M–Pd bimetallic acetates. Synthesis of $[Pd(\mu\text{-}OAc)_4Cu(OH_2)](AcOH)_2$ is found to be in competition with the trinuclear complex $Pd_2Cu(\mu\text{-}OAc)_6$ and Cu^{II} acetate however, such side reactions are not observed for the Ni or Zn analogues.[20] This additional $[Cu_2(\mu\text{-}OAc)_4]$ enhances the Cu ratio by affording some MOPs in which the M–Pd bimetallic node has been substituted by a Cu–Cu node.

An interesting difference arises in the crystal packing of the hetero-bimetallic MOPs compared to the $Cu_2(L)$ MOP material (L = 5-*tert*-butyl-1,3-benzenedicarboxylate). The previously reported $Cu_2(L)$ MOP material crystallises in the tetragonal space group *I*4/*mmm* under the conditions reported by Li *et al.* (DMA/methanol) with a body-centred cubic packing arrangement of the cuboctahedra.[25] The hetero-bimetallic paddlewheel structures reported here pack with a slight modification of this arrangement, presumably facilitated by subtle distortions of the cuboctahedral cage upon crystallisation, in which the cage centroids are translated slightly in the *a* and *b* axis directions. Intriguingly, hetero-bimetallic MOPs reported herein are isomorphous with the $Cu_2(L')$ MOPs (L' = 5-hydroxy-1,3-benzenedicarboxylate).

H_2 and N_2 77 K gas adsorption isotherms were performed to assess the permanent porosity of the bimetallic MOPs.

Initially, a careful activation procedure was carried out to ensure complete removal of the co-ordinated solvent molecules. We found that a previously reported method for activating structurally analogous materials (solvent exchange with MeOH followed by heating)[25] was unsatisfactory for the bimetallic MOPs. Indeed, ^{1}H NMR analysis of digested MOP samples activated by this method revealed the presence of significant amounts of DMA. To completely remove these coordinated solvent molecules MOP crystals were soaked in a solution of dry acetone for 7 days, followed by supercritical CO_2 drying and finally heating at 50˚C under vacuum for 3 hrs (heating above this temperature leads to visual darkening of the samples but thermogravimetric data indicates thermal stability to higher temperatures). By employing this activation protocol only trace amounts of DMA were detected by ^{1}H NMR spectroscopy (SI Figures 5-8). This procedure also led to dramatically increased H_2 and N_2 gas uptake for Cu_2(L) compared to previous reports.[25] It is noteworthy that subsequent to solvent removal powder X-ray diffraction experiments indicate that the MOPs are amorphous solids. Such 'crystalline-to-amorphous' transformations have been observed for other discrete porous materials and have been attributed to significant structural reorganisation upon solvent loss.[25, 26] Figure 2a shows the N_2 77 K gas adsorption isotherms collected for the MPd(L) and Cu_2(L) MOPs. The shape of the isotherms are best described as Type 1 with BET analysis of the isotherms yielding surface areas ranging from 200-1100 m^2/g. A noticeable hysteresis is observed in the desorption of CuPd(L) in addition to its considerably lower surface area with respect to its MPd(L) counterparts (M = Ni^{II}, Zn^{II}). This data further supports the relative instability of the CuPd(L) paddlewheel unit. As the MOPs lack precise long-range order the origin of porosity in these materials cannot be described from X-ray diffraction data, however, insights from the pore size distribution suggest a significant reduction in microporosity for Cu_2(L) and CuPd(L) (SI Figure 12) compared to NiPd(L) and ZnPd(L), which is consistent with their lower surface areas. Figure 2b shows the 77 K low pressure H_2 adsorption isotherms for Cu_2(L), NiPd(L), CuPd(L) and ZnPd(L). The isotherms for each MOP show reversible adsorption with steep uptake at low pressures. The H_2 uptake capacity of the MOPs range between 0.65 and 1.0 wt % at 77 K and 1 bar for CuPd(L) and NiPd(L), respectively. These data are consistent with the lower pore volume observed for the Cu_2(L) and CuPd(L) compared to the NiPd(L) and ZnPd(L) analogues. Isosteric heats of adsorption (Figure 3) were obtained from temperature independent virial fits to the isotherms, as described in the supporting information. A virial analysis was employed as it provided to the best fit to the adsorption isotherms exhibited by these disordered materials. The isosteric curves for ZnPd(L) and NiPd(L) indicate strong adsorption with initial Q_{st} values of -12.1 and -9.50 kJ/mol. As the hydrogen loading is increased, and the high affinity sites are saturated, the adsorption enthalpy decreases to approximately -7.5 kJ/mol. Such high adsorption enthalpies are competitive with exposed metal ion MOFs such as HKUST-1 and CPO-27-Ni, which have reported enthalpies of -10.1 and -13.5 kJ/mol, respectively.[27] These bimetallic MOPs show significantly stronger affinity for hydrogen than the Cu_2(L) structure which has an enthalpy of approximately -8 kJ/mol over the hydrogen loading range. In contrast to the other bimetallic MOPs the adsorption enthalpy of CuPd(L) shows a gradual decline from -10 kJ/mol to a value of -8.60 kJ/mol. The different enthalpy profile, compared to the other bimetallic MOPs, is most likely the result of the different pore structure present for CuPd(L) as evidenced by N_2 adsorption experiments. In this case the strong adsorption is consistent with small cavity sizes that bind hydrogen strongly by favourable 'wall-wall' overlaps rather than an open metal site.[5]

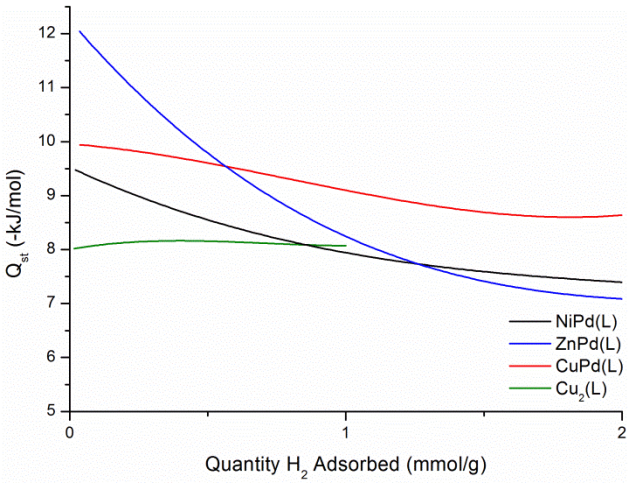

Figure 3. Coverage dependencies of the isosteric heats of adsorption for H_2 in the MOPs (calculated from 77 and 87 K isotherm data).

Preliminary DFT calculations were performed on modelled bimetallic paddlewheel clusters to provide insight into the hydrogen affinity observed in the bimetallic MOPs. Clusters comprised of Pd^{II}-M^{II} metals bridged by four formate ligands were optimized using Gaussian09 software with PBE0 and B97D3 functionals paired with the TZDVP basis set; a detailed description of this methodology is provided in the supporting information. The calculated parameters of water solvated optimised structures (SI Table 4), showed excellent agreement with the experimental data, with only subtle structural changes observed for the optimized desolvated MOPs. A strong anti-bonding component was observed for the highest occupied molecular orbitals (HOMOs) (SI Figure 15), which supports previous suggestions that the metal centres do not interact in the bimetallic paddlewheels.[24] For the NiPd(L) paddlewheel there are two possible spin states and comparison of a number of DFT functionals suggest that the high-spin (HS) complexes are more energetically favourable. However, we note that DFT methods must be used with caution in this application and as a result we calculated the hydrogen affinity for both spin states.[28] For the bimetallic series of formate clusters no appreciable interaction between the Pd^{II} ion and H_2 was found. In contrast, H_2 showed a strong affinity for each of the M^{II} sites that followed the trend: Ni(HS) > Zn > Cu > Ni(LS), (SI Table 9). Exceptionally high interaction energies, ca -11.4 kJ/mol, were observed for the Ni^{II} high-spin

structure. This can be explained by the partial occupation of σ* orbitals present that are able to stabilize the adsorption of H_2 through a Kubas-type bonding.[29] Indeed, this observation accounts for the substantially lower interaction energy (-2.04 kJ/mol) for low-spin Ni which cannot support Kubas-type bonding. The H_2–Zn and H_2–Cu interaction energies depend on the magnitude of partial positive charge on the metal (SI Table 11) that produces an attractive polarizing binding site for H_2. This theoretical data is in good agreement with the experimental results obtained for ZnPd(L) and NiPd(L) but not CuPd(L). The discrepancy between the calculated and experimental data for CuPd(L) suggests that the H_2 adsorption enthalpies are dominated by the pore structure rather than by specific interactions with the open metal sites. This is supported by the adsorption data which clearly demonstrates the porosity of CuPd(L) is distinct from the ZnPd(L) and NiPd(L) analogues.

In summary, a series of permanently porous heterometallic MOPs have been synthesized. The reaction of H_2L with bimetallic Pd^{II}–M^{II} (M = Ni, Cu or Zn) paddlewheel acetates produces discrete cage molecules of cuboctahedral geometry. Structural determination reveals preferential localisation of the Pd^{II} ions to the cage interior, while the relevant first row M^{II} species are predominantly positioned on the cage periphery. Careful activation of these molecules yields cages with an external surface decorated with co-ordinatively unsaturated metal sites poised for interaction with gas molecules in the solid-state. Indeed, H_2 gas adsorption experiments, combined with DFT modelling, show that these accessible M^{II} sites allow for high hydrogen binding energies in excess of -12 kJ/mol for NiPd(L). These novel framework building blocks are poised for further exploration. For example, we are currently assessing potential the Pd^{II} site for catalysis.

Notes and references

This research is supported by the Science and Industry Endowment Fund (SIEF). CJD and CJS would like to acknowledge the Australian Research Council for funding FT100100400 and FT0991910, respectively. Aspects of this research were undertaken on the MX beamlines at the Australian Synchrotron, Victoria, Australia.

1 (a) B. L. Chen, N. W. Ockwig, A. R. Millward, D. S. Contreras and O. M. Yaghi, *Angew. Chem. Int. Ed.*, **44**, 4745-4749. B. L. Chen, N. W. Ockwig, A. R. Millward, D. S. Contreras and O. M. Yaghi, *Angew. Chem. Int. Ed.*, 2005, **44**, 4745-4749. (b) S. Xiang, W. Zhou, J. M. Gallegos, Y. Liu and B. Chen, *J. Am. Chem. Soc.*, 2009, **131**, 12415-12419. (c) Z. Zhang, S. Xiang and B. Chen, *CrystEngComm*, 2011, **13**, 5983-5992. (d) M. Dincă and J. R. Long, *Angew. Chem. Int. Ed.*, 2008, **47**, 6766-6779. (e) O. Kozachuk, I. Luz, F. X. Llabrés i Xamena, H. Noei, M. Kauer, H. B. Albada, E. D. Bloch, B. Marler, Y. Wang, M. Muhler and R. A. Fischer, *Angew. Chem. Int. Ed.*, 2014, **53**, 7058-7062. (f) A. A. Talin, A. Centrone, A. C. Ford, M. E. Foster, V. Stavila, P. Haney, R. A. Kinney, V. Szalai, F. El Gabaly, H. P. Yoon, F. Léonard and M. D. Allendorf, *Science*, 2013, *10.1126/science.1246738*. (g) P. Mahato, A. Monguzzi, N. Yanai, T. Yamada and N. Kimizuka, *Nat. Mater.*, 2015, **14**, 924-930. (h) K. Liang, R. Ricco, C. M. Doherty, M. J. Styles, S. Bell, N. Kirby, S. Mudie, D. Haylock, A. J. Hill, C. J. Doonan and P. Falcaro, *Nat. Commun.*, 2015, **6**, 7240.

2 N. L. Rosi, J. Kim, M. Eddaoudi, B. Chen, M. O'Keeffe and O. M. Yaghi, *J. Am. Chem. Soc.*, 2005, **127**, 1504-1518.

3 E. Tsivion, J. R. Long and M. Head-Gordon, *J. Am. Chem. Soc.*, 2014, **136**, 17827-17835.

4 S. Bordiga, L. Regli, F. Bonino, E. Groppo, C. Lamberti, B. Xiao, P. S. Wheatley, R. E. Morris and A. Zecchina, *Phys. Chem. Chem. Phys.*, 2007, **9**, 2676-2685.

5 J. L. C. Rowsell and O. M. Yaghi, *J. Am. Chem. Soc.*, 2006, **128**, 1304-1315.

6 O. K. Farha and J. T. Hupp, *Acc. Chem. Res.*, 2010, **43**, 1166-1175.

7 J. J. Perry IV, J. A. Perman and M. J. Zaworotko, *Chem. Soc. Rev.*, 2009, **38**, 1400-1417.

8 S. L. James, *Chem. Soc. Rev.*, 2003, **32**, 276-288.

9 9. F. N. Dai, H. Y. He, D. L. Gao, F. Ye, X. L. Qiu and D. F. Sun, *CrystEngComm*, 2009, **11**, 2516-2522.

10 J. R. Li, R. J. Kuppler and H. C. Zhou, *Chem. Soc. Rev.*, 2009, **38**, 1477-1504.

11 R. Yepez, S. Garcia, P. Schachat, M. Sanchez-Sanchez, J. H. Gonzalez-Estefan, E. Gonzalez-Zamora, I. A. Ibarra and J. Aguilar-Pliego, *New J. Chem.*, 2015, **39**, 5112-5115.

12 M. Položij, E. Pérez-Mayoral, J. Čejka, J. Hermann and P. Nachtigall, *Cat. Today*, 2013, **204**, 101-107.

13 S. Naito, T. Tanibe, E. Saito, T. Miyao and W. Mori, *Chem. Lett.*, 2001, **30**, 1178-1179.

14 O. Kozachuk, K. Yusenko, H. Noei, Y. Wang, S. Walleck, T. Glaser and R. A. Fischer, *Chem. Comm.*, 2011, **47**, 8509-8511.

15 Y. Ke, D. J. Collins and H.-C. Zhou, *Inorg. Chem.*, 2005, **44**, 4154-4156.

16 E.-Y. Choi, P. M. Barron, R. W. Novotny, H.-T. Son, C. Hu and W. Choe, *Inorg. Chem.*, 2009, **48**, 426-428.

17 K. Tan, P. Canepa, Q. Gong, J. Liu, D. H. Johnson, A. Dyevoich, P. K. Thallapally, T. Thonhauser, J. Li and Y. J. Chabal, *Chem. Mat.*, 2013, **25**, 4653-4662.

18 Q. Yao, J. Sun, K. Li, J. Su, M. V. Peskov and X. Zou, *Dalton Trans.*, 2012, **41**, 3953-3955.

19 M. Dincă and J. R. Long, *J. Am. Chem. Soc.*, 2007, **129**, 11172-11176.

20 N. S. Akhmadullina, N. V. Cherkashina, N. Y. Kozitsyna, I. P. Stolarov, E. V. Perova, A. E. Gekhman, S. E. Nefedov, M. N. Vargaftik and I. I. Moiseev, *Inorg. Chim. Acta*, 2009, **362**, 1943-1951.

21 P. Day, A. F. Orchard, A. J. Thomson and R. J. P. Williams, *J. Chem. Phys.*, 1965, **42**, 1973-1981.

22 A. J. Blake, N. R. Champness, P. Hubberstey, W.-S. Li, M. A. Withersby and M. Schröder, *Coord. Chem. Rev.*, 1999, **183**, 117-138.

23 T. Akitsu, *Polyhedron*, 2007, **26**, 2527-2535.

24 A. A. Markov, A. P. Klyagina, S. P. Dolin, N. S. Akhmadullina, N. Y. Kozitsyna, N. V. Cherkashina, S. E. Nefedov, M. N. Vargaftik and I. I. Moiseev, *Russ. J. Inorg. Chem.*, 2009, **54**, 885-892.

25 J.-R. Li and H.-C. Zhou, *Nat. Chem.*, 2010, **2**, 893-898.

26 F.-R. Dai, U. Sambasivam, A. J. Hammerstrom and Z. Wang, *J. Am. Chem. Soc.*, 2014, **136**, 7480-7491.

27 J. G. Vitillo, L. Regli, S. Chavan, G. Ricchiardi, G. Spoto, P. D. C. Dietzel, S. Bordiga and A. Zecchina, *J. Am. Chem. Soc.*, 2008, **130**, 8386-8396.

28 J. Harvey, in *Principles and Applications of Density Functional Theory in Inorganic Chemistry I*, Springer Berlin Heidelberg, 2004, 112, 4, 151-184.

29 G. J. Kubas, *Chem. Rev.*, 2007, **107**, 4152-4205.

